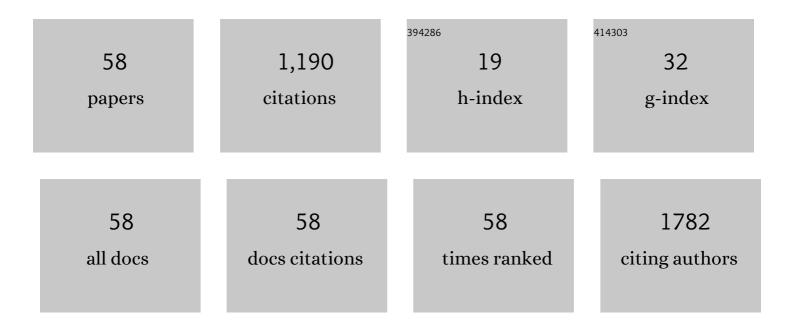
MÃ;ria ÄŒaploviÄovÃ;

List of Publications by Year in descending order

Source: https://exaly.com/author-pdf/9463912/publications.pdf Version: 2024-02-01



#	Article	IF	CITATIONS
1	Effect of Multiply Twinned Ag(0) Nanoparticles on Photocatalytic Properties of TiO2 Nanosheets and TiO2 Nanostructured Thin Films. Nanomaterials, 2022, 12, 750.	1.9	3
2	Contribution of photocatalytic and Fenton-based processes in nanotwin structured anodic TiO ₂ nanotube layers modified by Ce and V. Dalton Transactions, 2022, 51, 10763-10772.	1.6	4
3	Fe3O4-PEI Nanocomposites for Magnetic Harvesting of Chlorella vulgaris, Chlorella ellipsoidea, Microcystis aeruginosa, and Auxenochlorella protothecoides. Nanomaterials, 2022, 12, 1786.	1.9	11
4	Effect of Gallium and Boron doping on dielectric and conductivity properties of ZnO sintered from nanoparticles of different morphology in THz region. Colloids and Surfaces A: Physicochemical and Engineering Aspects, 2021, 611, 125896.	2.3	0
5	ZnO nanoparticles as photodegradation agent controlled by morphology and boron doping. Catalysis Science and Technology, 2021, 11, 2167-2185.	2.1	13
6	Formation of CuCrCoFeNiO high entropy alloy thin films by rapid thermal processing of Cu/CrNiO/FeCo multilayers. Surface and Coatings Technology, 2021, 405, 126563.	2.2	7
7	Effect of Sub-Zero Treatments and Tempering on Corrosion Behaviour of Vanadis 6 Tool Steel. Materials, 2021, 14, 3759.	1.3	9
8	Catalytic graphitization of single-crystal diamond. Carbon, 2021, 185, 300-313.	5.4	24
9	Ce ion surface-modified TiO ₂ aerogel powders: a comprehensive study of their excellent photocatalytic efficiency in organic pollutant removal. New Journal of Chemistry, 2021, 45, 4174-4184.	1.4	7
10	Thermally induced structural evolution and age-hardening of polycrystalline V1–xMoxN (xÂâ‰^Â0.4) thin films. Surface and Coatings Technology, 2021, 405, 126723.	2.2	11
11	Ti3+ doped anodic single-wall TiO2 nanotubes as highly efficient photocatalyst. Electrochimica Acta, 2020, 331, 135374.	2.6	38
12	Dehydroaromatization of methane over Mo/ZSM-5 zeolites: influence of aluminum distribution in the crystals. Reaction Kinetics, Mechanisms and Catalysis, 2020, 131, 889-904.	0.8	3
13	Polarization dependent photoluminescence and optical anisotropy in CuPtB-ordered dilute GaAs1–xBix alloys. Journal of Applied Physics, 2020, 128, 195106.	1.1	8
14	Toward BaSi 2 /Si Heterojunction Thinâ€Film Solar Cells: Insights into Heterointerface Investigation, Barium Depletion, and Silicideâ€Mediated Silicon Crystallization. Advanced Materials Interfaces, 2020, 7, 2000887.	1.9	6
15	Green synthesis of stable nanocolloids of monodisperse silver and gold nanoparticles using natural polyphenols from fruits of Sambucus nigra L Applied Nanoscience (Switzerland), 2020, 10, 4545-4558.	1.6	17
16	Ni-mediated reactions in nanocrystalline diamond on Si substrates: the role of the oxide barrier. RSC Advances, 2020, 10, 8224-8232.	1.7	6
17	GaAs1-xBix growth on Ge: anti-phase domains, ordering, and exciton localization. Scientific Reports, 2020, 10, 2002.	1.6	10
18	Atomic-Resolution EDX, HAADF, and EELS Study of GaAs1-xBix Alloys. Nanoscale Research Letters, 2020, 15, 121.	3.1	14

ΜΑ̃; RIA ÄŒAPLOVIÄOVÃ;

#	Article	IF	CITATIONS
19	Changes in microstructure of ledeburitic tool steel due to vacuum austenitizing and quenching, sub-zero treatments at â~'140°C and tempering. Vacuum, 2019, 170, 108977.	1.6	21
20	Covalent Diamond–Graphite Bonding: Mechanism of Catalytic Transformation. ACS Nano, 2019, 13, 4621-4630.	7.3	38
21	Tuning the orientation of few-layer MoS ₂ films using one-zone sulfurization. RSC Advances, 2019, 9, 29645-29651.	1.7	24
22	Structural, surface and magnetic properties of chalcogenide Co9S8 nanoparticles prepared by mechanochemical synthesis. Journal of Alloys and Compounds, 2018, 745, 863-867.	2.8	15
23	Enhanced photocatalytic activity of hydrogenated and vanadium doped TiO2 nanotube arrays grown by anodization of sputtered Ti layers. Applied Surface Science, 2018, 434, 1257-1265.	3.1	44
24	Structure of superconducting MgB2 thin films prepared by vacuum evaporation and ex-situ annealing in Ar and O2 atmospheres. Applied Surface Science, 2018, 461, 233-241.	3.1	4
25	Degradation of Al4C3 Due to Atmospheric Humidity. Jom, 2018, 70, 2378-2384.	0.9	3
26	The real structure of ε-Ga ₂ O ₃ and its relation to κ-phase. CrystEngComm, 2017, 19, 1509-1516.	1.3	227
27	Heterotrophic Bacterial Leaching of Zinc and Arsenic from Artificial Adamite. Water, Air, and Soil Pollution, 2017, 228, 1.	1.1	11
28	Mineralogy and Surface Chemistry of Alberta Oil Sands: Relevance to Nonaqueous Solvent Bitumen Extraction. Energy & Fuels, 2017, 31, 8910-8924.	2.5	9
29	Nanoscale iron particles formed from the metalloprotein-like structures prepared using ferrous ions in the presence of sodium glutamate and bovine serum albumin. Monatshefte Für Chemie, 2017, 148, 2019-2029.	0.9	5
30	Formation of silica aggregates in sorghum root endodermis is predetermined by cell wall architecture and development. Annals of Botany, 2017, 120, 739-753.	1.4	63
31	Terahertz time domain detection of imidazolium ionic liquid reactivity in nanohybrid materials based on Kaolinite and Halloysite. Applied Clay Science, 2017, 135, 475-484.	2.6	5
32	Delimitation of European CrepidotusÂstenocystis as different from the North American species C.Âbrunnescens (Inocybaceae, Agaricales). Phytotaxa, 2017, 328, 127.	0.1	4
33	XRD, SAXS, and PALS investigations of three different polymers reinforced with tetraoctylammonium exchanged montmorillonite. International Journal of Polymer Analysis and Characterization, 2016, 21, 524-536.	0.9	5
34	Characterization of clays from the CorumbataÃ-formation used as raw material for ceramic industry in the Santa Gertrudes district, São Paulo, Brazil. Applied Clay Science, 2016, 132-133, 232-242.	2.6	19
35	Photo-catalytic inactivation of an <i>Enterococcus</i> biofilm: the anti-microbial effect of sulphated and europium-doped titanium dioxide nanopowders. FEMS Microbiology Letters, 2016, 363, fnw051.	0.7	8
36	Photocatalytic properties and selective antimicrobial activity of TiO2(Eu)/CuO nanocomposite. Applied Surface Science, 2016, 371, 538-546.	3.1	31

ΜΑ̃; RIA ÄŒAPLOVIÄOVÃ;

#	Article	IF	CITATIONS
37	CdS/ZnS nanocomposites: from mechanochemical synthesis to cytotoxicity issues. Materials Science and Engineering C, 2016, 58, 1016-1023.	3.8	34
38	Mechanochemical synthesis of InAs nanocrystals. Materials Letters, 2015, 159, 474-477.	1.3	7
39	Influence of Grinding and Sonication on the Crystal Structure of Talc. Clays and Clay Minerals, 2015, 63, 311-327.	0.6	20
40	The Effect of Salivary Gland Extract of Lucilia sericata Maggots on Human Dermal Fibroblast Proliferation within Collagen/Hyaluronan Membrane In Vitro. Advances in Skin and Wound Care, 2015, 28, 221-226.	0.5	11
41	Iron oxides in human spleen. BioMetals, 2015, 28, 913-928.	1.8	26
42	Nontronites as catalyst for synthesis of carbon nanotubes by catalytic chemical vapor deposition Applied Clay Science, 2015, 114, 170-178.	2.6	9
43	The influence of molybdenum loading on activity of ZSM-5 zeolite in dehydroaromatization of methane. Microporous and Mesoporous Materials, 2015, 212, 146-155.	2.2	35
44	Arsenic sulfide nanoparticles prepared by milling: properties, free-volume characterization, and anti-cancer effects. Journal of Materials Science, 2015, 50, 1973-1985.	1.7	50
45	Unexpected formation of Ag2SO4 microparticles from Ag2S nanoparticles synthesised using poplar leaf extract. Environmental Chemistry Letters, 2014, 12, 551-556.	8.3	5
46	The dual role of sulfur-containing amino acids in the synthesis of IV–VI semiconductor nanocrystals: a mechanochemical approach. Faraday Discussions, 2014, 170, 169-179.	1.6	12
47	Photocatalytic and photodisinfectant activity of sulfated and Eu doped anatase against clinically important microorganisms. Ceramics International, 2014, 40, 5745-5756.	2.3	16
48	Hydrogen production by photocatalytic ethanol reforming using Eu- and S-doped anatase. Applied Surface Science, 2014, 305, 665-669.	3.1	15
49	Electric-field-induced structuring and rheological properties of kaolinite and halloysite. Applied Clay Science, 2013, 77-78, 1-9.	2.6	34
50	Structural Incorporation of As ⁵⁺ into Hematite. Environmental Science & Technology, 2013, 47, 9140-9147.	4.6	70
51	Structural Evolution of Sputtered Indium Oxide Thin Films. Journal of Electrical Engineering, 2010, 61, 382-385.	0.4	14
52	Mechanochemical-molten salt synthesis of Na2Ti6O13 nanobelts. Materials Research Bulletin, 2010, 45, 621-627.	2.7	16
53	Carbon Nanostructures Grown on Fe-Cr-Al Alloy. Journal of Electrical Engineering, 2010, 61, 373-377.	0.4	2
54	Potentialities of scanning electron microscopy and EDX analysis in bullet wounds. Romanian Journal of Legal Medicine, 2010, 18, 225-230.	0.3	7

#	Article	IF	CITATIONS
55	Photoactivity of mechanochemically prepared nanoparticulate titanium dioxide investigated by EPR spectroscopy. Journal of Photochemistry and Photobiology A: Chemistry, 2009, 206, 177-187.	2.0	20
56	Partial Dissolution of Glauconitic Samples: Implications for the Methodology of K-Ar and Rb-Sr Dating. Clays and Clay Minerals, 2009, 57, 531-554.	0.6	30
57	Growth of carbon nanofibers and related structures by combined method of plasma enhanced chemical vapor deposition and aerosol synthesis. Vacuum, 2008, 82, 805-813.	1.6	4
58	Analysis of magnetron sputtered boron oxide films. Thin Solid Films, 2007, 515, 8723-8727.	0.8	26